

## ELECTRONIC SUPPLEMENTARY INFORMATION

### Lead and zinc concentrations in household dust and toenails of the residents (Estarreja, Portugal): a source-pathway-fate model

A. Paula Marinho Reis<sup>a\*</sup>, M. Cave<sup>b</sup>, A. J. Sousa<sup>c</sup>, J. Wragg<sup>b</sup>, M. J. Rangel<sup>d</sup>, A. R. Oliveira<sup>d</sup>, C. Patinha<sup>a</sup>, F. Rocha<sup>a</sup>, T. Orsiere<sup>c</sup> and Y. Noack<sup>f</sup>

<sup>a</sup> GEOBIOTEC, Departamento de Geociências, Universidade de Aveiro, Campus Universitário de Santiago, 3810-193 Aveiro, Portugal

<sup>b</sup> British Geological Survey, Keyworth, Nottingham, NG12 5GG, United Kingdom

<sup>c</sup> CERENA, Instituto Superior Técnico, Av. Rovisco Pais, 1049-001, Lisboa, Portugal

<sup>d</sup> Departamento de Geociências, Universidade de Aveiro, Campus Universitário de Santiago, 3810-193 Aveiro, Portugal

<sup>e</sup> Aix Marseille Univ, Avignon Université, CNRS, IRD, IMBE, Equipe Biomarqueurs Environnement Santé, Faculté de Médecine, Marseille, France

<sup>f</sup> Aix Marseille University, CNRS, IRD, INRA, Coll France, CEREGE, Aix-en-Provence, France

\* corresponding author; email: [pmarinho@ua.pt](mailto:pmarinho@ua.pt)

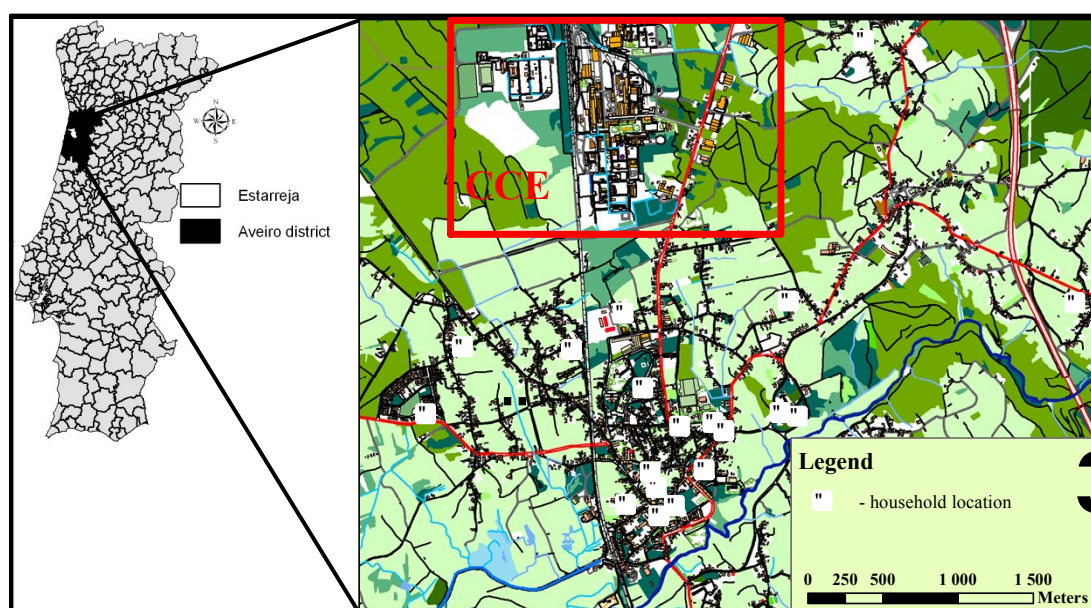


Fig. S1. The framing of the study area within the country and location of the sampled private homes. The red rectangle locates the chemical complex of Estarreja (CCE).

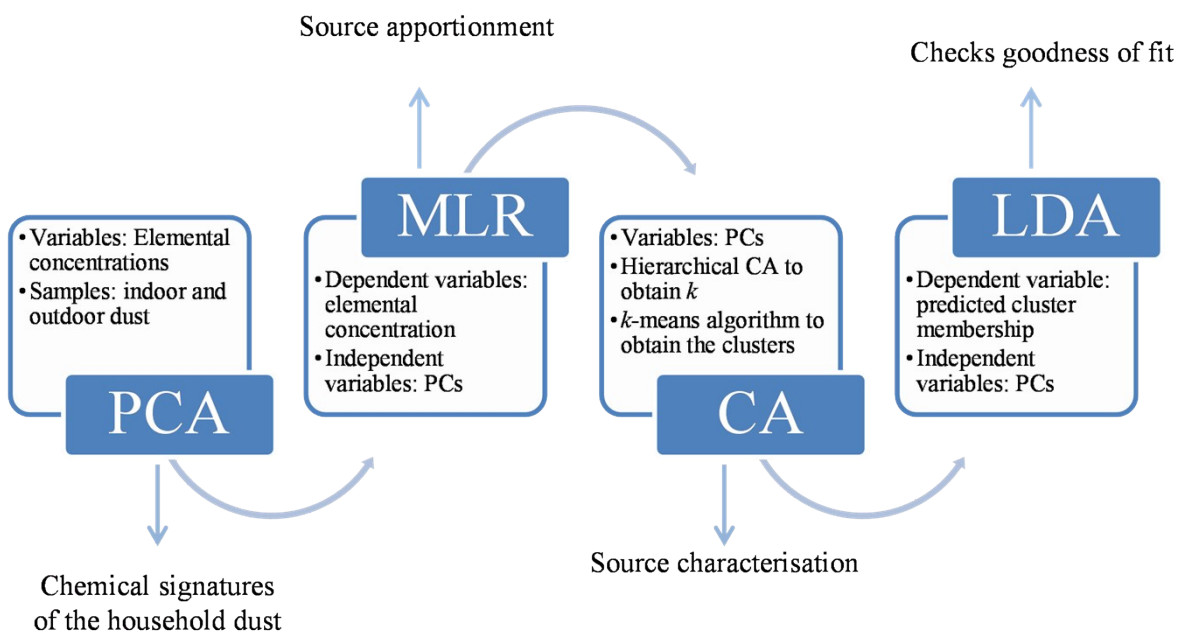


Fig. S2. Flow diagram summarising the statistical methodology developed.

Table S1. Summary statistics for near total concentrations determined both in indoor and outdoor dust samples (n=37).

Element	MDL <sup>a</sup>	Dust	Minimum	Median	Mean $\pm$ SD	Maximum
Pb	0.01 mg kg <sup>-1</sup>	IN	53	118	174 $\pm$ 250	1180
		OUT	24	74	121 $\pm$ 155	714
Zn	0.1 mg kg <sup>-1</sup>	IN	582	1110	1349 $\pm$ 1020	5210
		OUT	237	586	1265 $\pm$ 1789	7030

MDL: minimum detection limit; SD: standard deviation; IN: indoor dust samples; OUT: outdoor dust samples; \*: p < 0.05; \*\*: p < 0.01

Table S2. Bioaccessible concentrations of Pb and Zn determined in the stomach stage of the UBM, and the calculated bioaccessible fraction (BAF).

Sample ID	Pb_stomach (mg kg <sup>-1</sup> )	Pb_BAF (%)	Zn_stomach (mg kg <sup>-1</sup> )	Zn_BAF(%)
2	52	67	1260.3	83
3	100	68	951.2	86
8	78	54	826.6	84
10	74	63	1220.4	86
12	218	82	4446.0	85
13	57	67	852.3	87
15	245	21	657.6	66
16	165	72	1443.2	91
17	66	43	946.4	84
Mean ± SD	117 ± 73	60 ± 18	1400 ± 1168	84 ± 7
Median	78	67	951	85

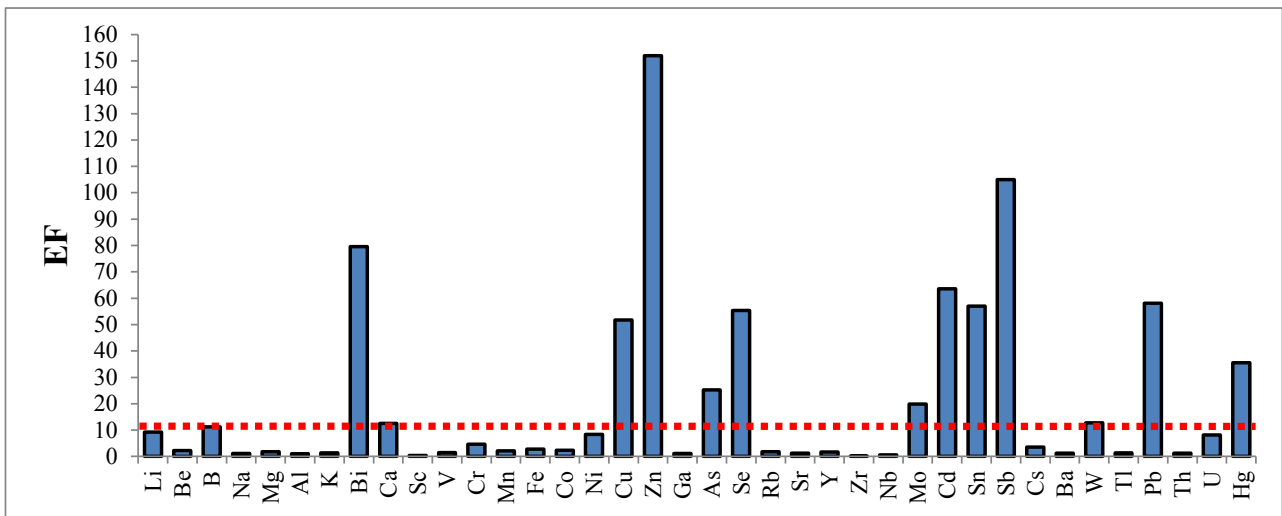
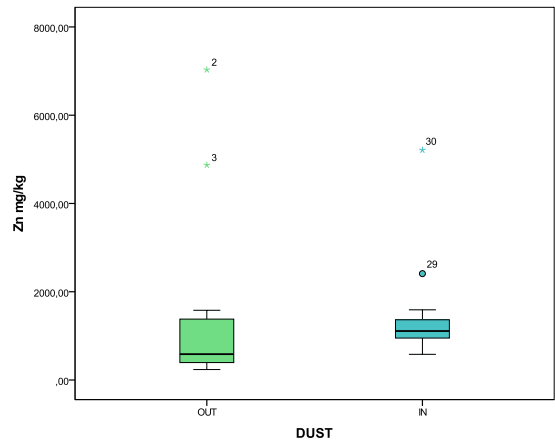
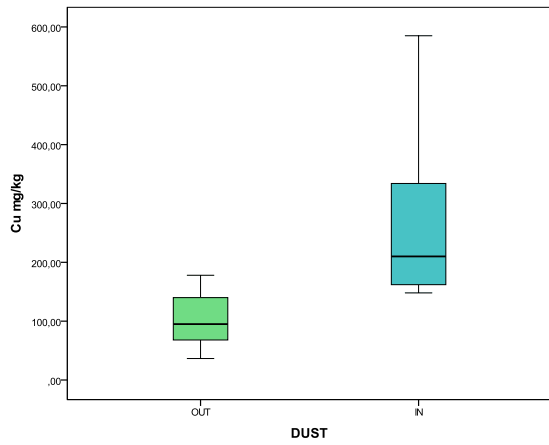
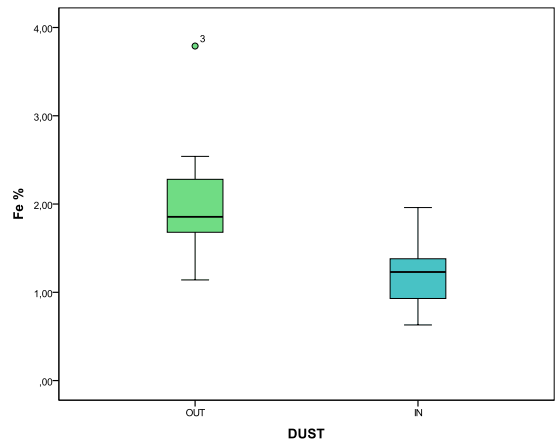
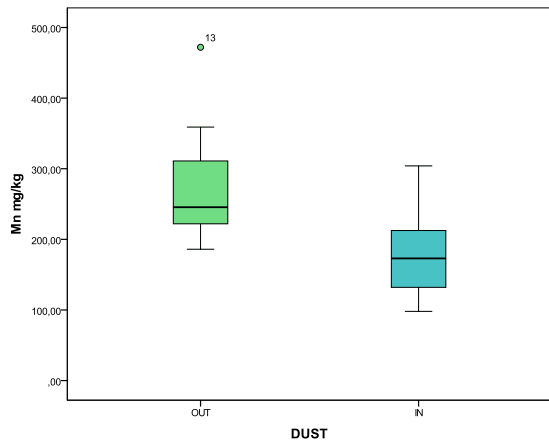
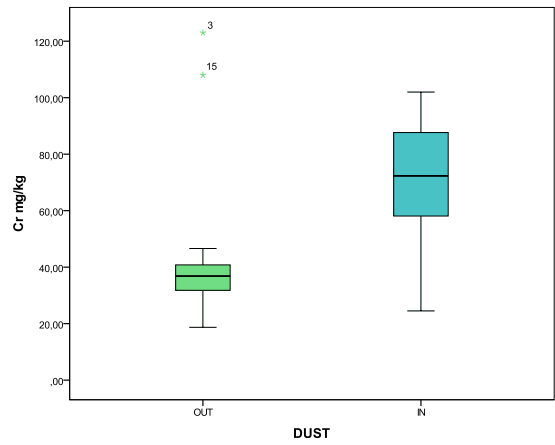
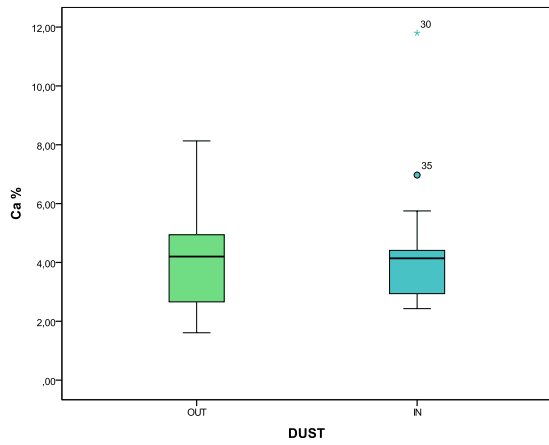
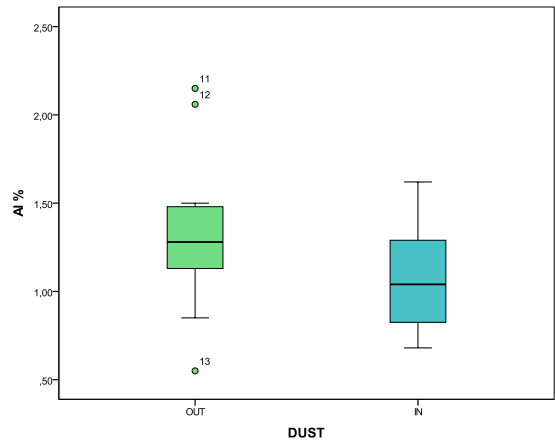
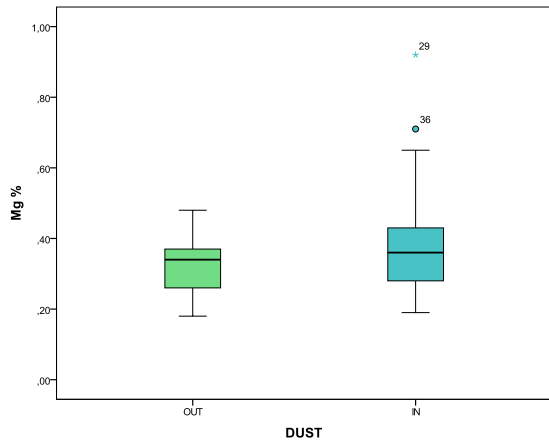


Fig. S3. Enrichment factors for elements detected with ICP-MS.

Table S3. Eigenvalues, % of the total variance and loadings of active (in bold) and supplementary variables in the four principal components under study.

	PC1	PC2	PC3	PC4
<b>B</b>	0.802	-0.180	-0.065	0.420
<b>Bi</b>	0.686	0.216	0.152	-0.482
<b>Ca</b>	0.282	-0.381	-0.105	-0.495
<b>Cu</b>	0.913	0.033	-0.023	-0.073
<b>Zn</b>	0.664	-0.322	0.077	-0.448
<b>As</b>	-0.596	-0.325	0.555	-0.070
<b>Se</b>	0.290	-0.655	0.359	0.173
<b>Mo</b>	0.416	0.244	0.766	-0.005
<b>Cd</b>	0.773	-0.361	-0.203	0.109
<b>Sn</b>	0.796	0.281	-0.014	-0.209
<b>Sb</b>	0.583	0.276	0.251	0.433
<b>W</b>	0.692	0.451	0.076	0.066
<b>Pb</b>	0.467	-0.705	-0.029	0.180
<b>Hg</b>	0.800	0.116	-0.203	0.134
Li	-0.477	-0.147	0.442	-0.010
Be	-0.397	-0.416	0.441	0.065
Na	0.882	0.200	-0.227	0.205
Mg	0.269	0.163	0.109	0.153
Al	-0.068	-0.482	0.365	0.262
K	0.798	0.023	-0.070	0.170
Sc	-0.590	-0.174	0.401	-0.161
V	-0.367	-0.440	0.430	-0.037
Cr	0.745	0.139	0.202	0.290
Mn	-0.410	-0.257	0.472	-0.062
Fe	-0.361	-0.445	0.552	-0.001
Co	0.094	-0.128	0.608	0.090
Ni	0.862	0.040	0.050	0.078
Ga	-0.379	-0.369	0.523	0.182
Rb	-0.356	-0.219	0.510	-0.013
Sr	0.582	-0.337	0.162	-0.036
Y	-0.579	-0.281	0.413	-0.188
Zr	0.187	0.218	0.025	0.002
Nb	-0.028	-0.321	0.488	-0.070
Ag	0.813	0.233	-0.298	0.173
Cs	-0.493	-0.179	0.555	-0.080
Ba	-0.272	-0.074	0.076	-0.310
Au	0.863	0.050	-0.238	0.237
Tl	-0.461	-0.407	0.485	-0.027
Th	-0.714	0.048	0.368	-0.275
U	-0.629	-0.106	0.347	-0.154
La	-0.349	-0.040	0.124	-0.035
Ce	-0.450	-0.064	0.189	-0.061
Eigenvalue	5.990	1.920	1.220	1.190
% of the total variance	42.76	13.72	8.72	8.51
% cumulative variance	42.76	56.49	65.20	73.71



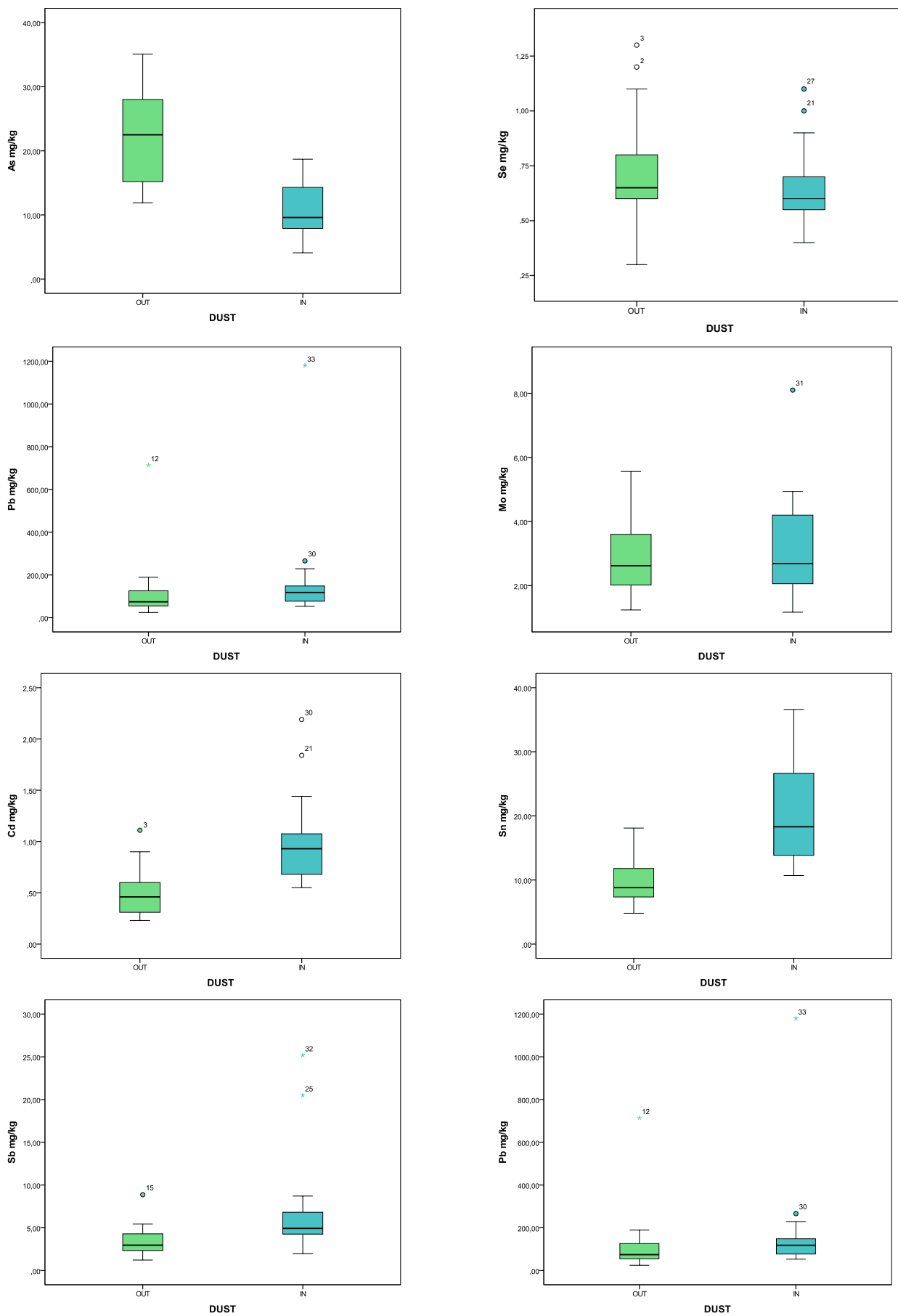


Figure S4. Box-plots displaying total concentrations of the chemical elements used in multivariate analysis, in outdoor (in green) and indoor (in blue) dust samples.

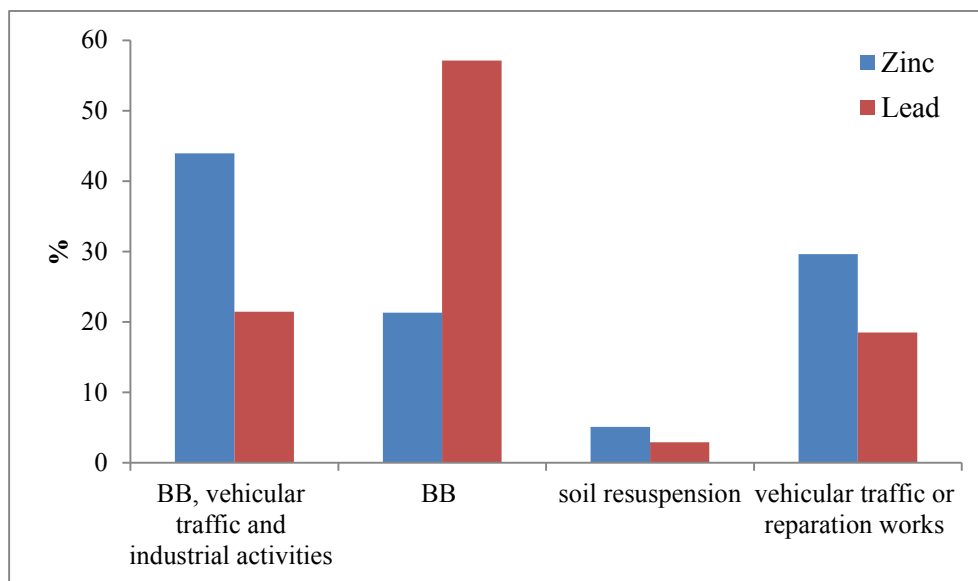


Figure S5. Source apportionment of total dust contents of Pb and Zn. BB- biomass burning

Table S4. Cluster profiles and mean principal component values obtained from the *k*-means cluster analysis.

	Cluster					Mean PC values	
	1	2	3	4	5	positive scores	negative scores
PC1	.25	.58	.72	.28	-.77	.45	-0.74
PC2	.30	.23	-.74	-.44	.03	.26	-0.30
PC3	-.32	.06	-.69	.10	.07	.26	-0.22
PC4	.17	-.12	-.81	.22	-.05	.20	-0.21

Table S5. Sample classification matrix for the linear discriminant analysis model of the CA predicted membership.

	Cluster I	Cluster II	Cluster III	Cluster IV	Cluster V	Total
Cluster I	5	0	0	0	0	5
Cluster II	1	9	0	0	0	10
Cluster III	0	0	1	0	0	1
Cluster IV	0	0	0	8	0	8
Cluster V	0	0	0	0	13	13

Table S6: Results of the random forest (RF) analysis; the variables are listed according to their increasing importance to predict toenail Pb and Zn.

PTE	Predictors in the RF model	% Variance explained
Pb	Age group, indoor dust Se contents, water used to cook, wash and bath, area of the house, indoor dust Cd contents, home-reared poultry, indoor dust Sn contents	29%
Zn	House age, location, age group, Zn indoor dust contents and occurrence of recent repair	32%



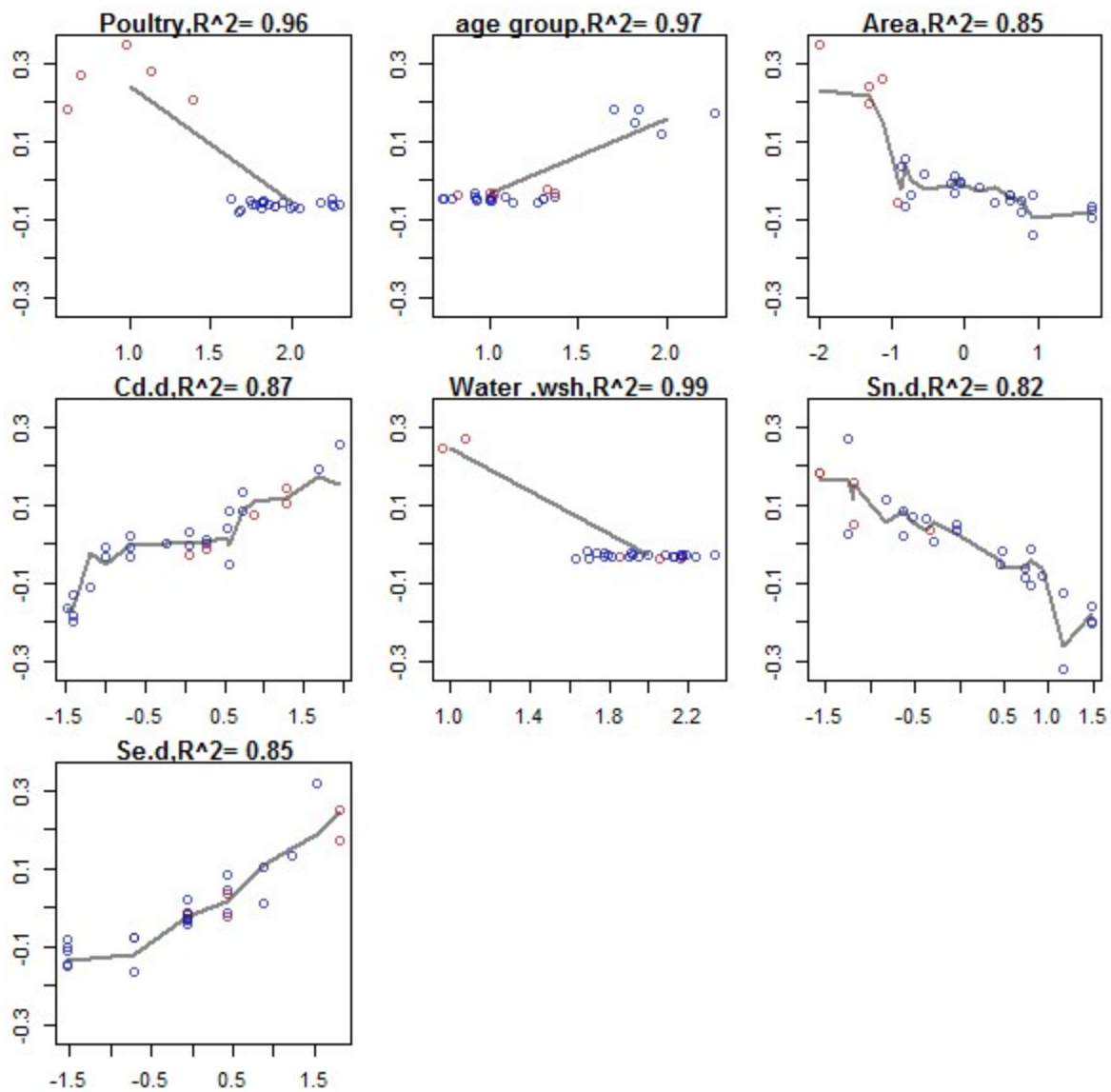


Figure S6. Sensitivity analysis of the RF model for Pb; the effect of parameters on toenail Pb predictions is coloured by poultry; home-reared poultry is a binary variable (1=yes; 2=no); age group is a binary variable (1=adult; 2=children); the water used to cook, shower and wash has four categories (1=fountain; 2=spring; 3- well water; 4- tap water); other variables are quantitative. The y-axis represents transformed Pb concentrations (BoxCox transformation followed by mean centering and scaling to unit variance) in toenails and the x-axis of each individual predictor is its transformed value showing, according to the RF model, how each individual predictor affects the Pb in toenails of the participants.

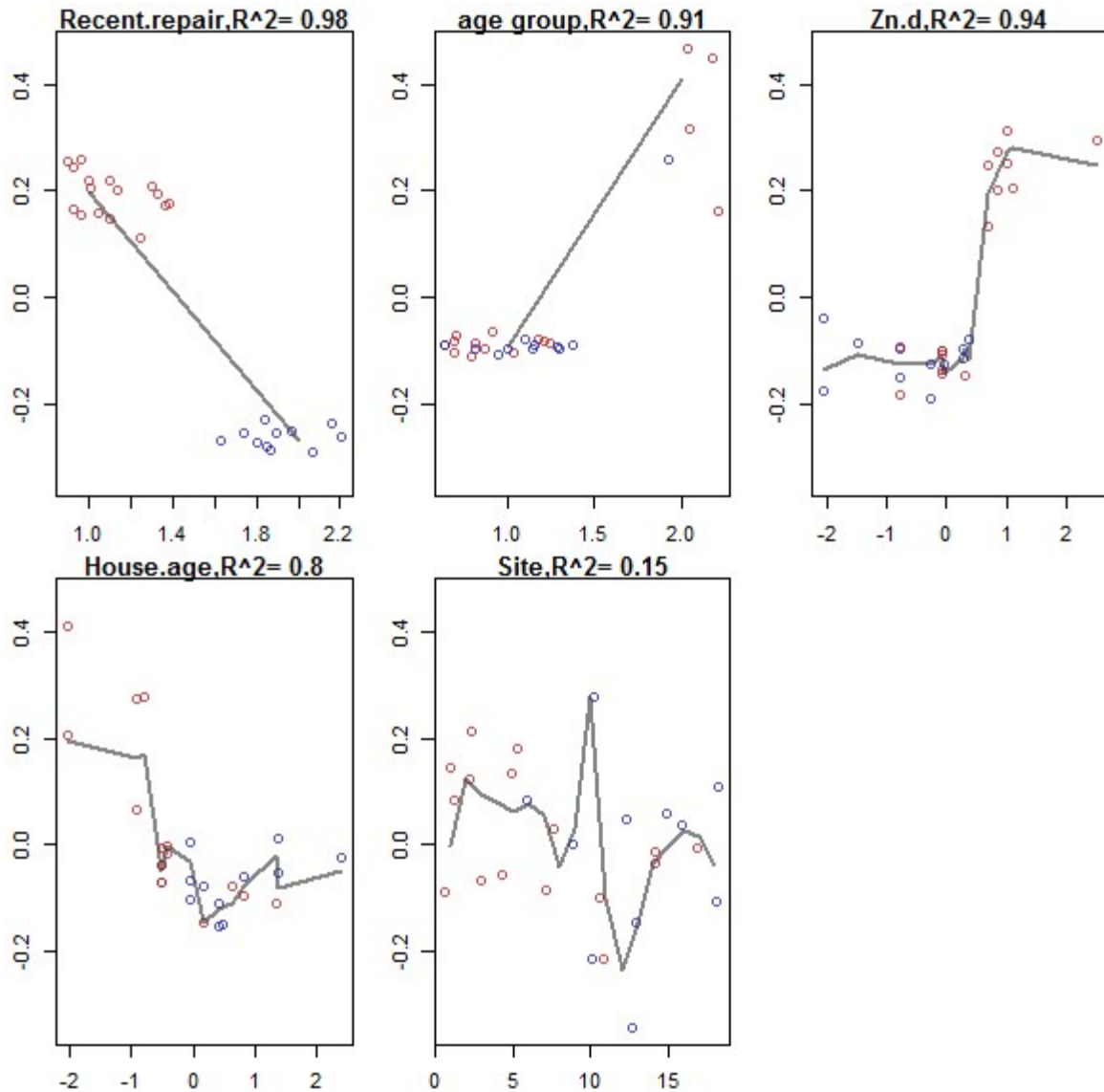
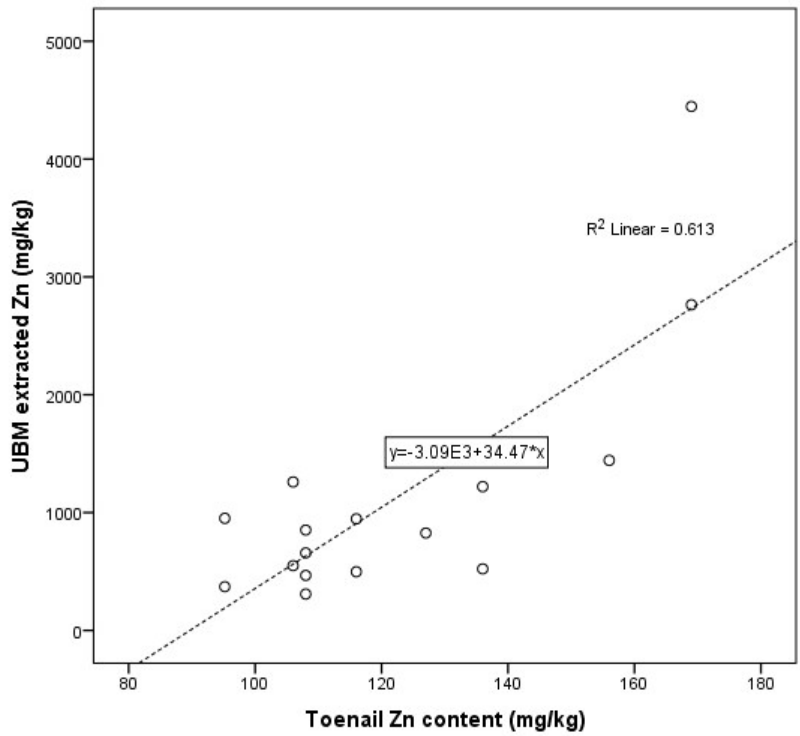
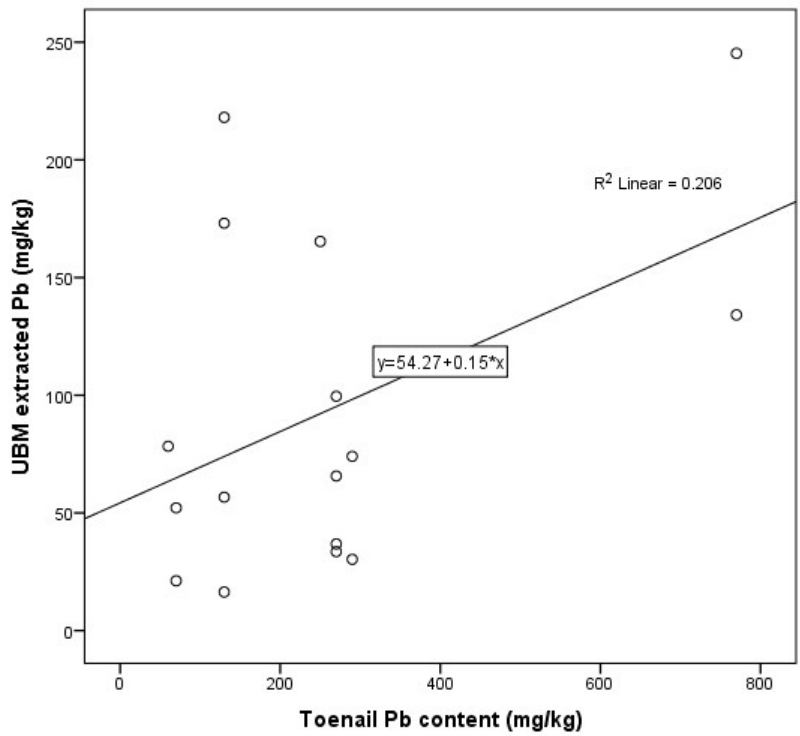


Figure S7. Sensitivity analysis of the RF model for Zn; the effect of the parameters on toenail Pb predictions is coloured by the occurrence of recent reparation works in the house; recent repair is a binary variable (1=yes; 2=no). The y-axis represents transformed Zn concentrations (BoxCox transformation followed by mean centering and scaling to unit variance) in toenail and the x-axis of each individual predictor is its transformed value showing, according to the RF model, how each individual predictor affects the Zn in toenails of the participants.



a



b

Figure S8. XY graph of toenail contents vs bioaccessible concentrations in the indoor dust and coefficient of determination ( $R^2$ ) for Zn (graph a) and Pb (graph b).